

## High-speed steel tool wear during wood cutting in the presence of high-temperature corrosion and mineral contamination

Bolesław Porankiewicz · Piotr Iskra · Jakub Sandak ·  
Chiaki Tanaka · Karol Józwiak

Received: 9 November 2005 / Published online: 14 July 2006  
© Springer-Verlag 2006

**Abstract** Dulling of high-speed steel (HSS) cutting tools after milling five wood species has been analyzed. The wood investigated varied in mineral contamination, high-temperature corrosivity (HTC) and density ( $D$ ). Experiments performed proved that up to date methods for evaluation of mineral contamination in wood should be improved. A new pipe-like form of mineral contamination particles was evidenced. The correlation between the presence of 3D aggregates of silica in wood and high content of K and Ca in the ash was established. Employing multivariable theoretical simulation method, the combined effect of mineral contamination, HTC and wood density on the tool dullness appeared to be a reasonable explanation of the results obtained.

---

B. Porankiewicz (✉)  
Faculty of Wood Technology, August Cieszkowski Agricultural University of Poznań,  
Wojska Polskiego 38/42, 60-637 Poznan, Poland  
e-mail: poranek@amu.edu.pl

P. Iskra  
Department of Natural Resources Process Engineering, Shimane University,  
690-8504 Matsue, Japan

J. Sandak  
Trees and Timber Research Institute IV ALSA/CNR, V.la. Biassi 75,  
38010 S Michele TN, Italy

C. Tanaka  
Department of Environmental Science and Technology, Faculty of Agriculture,  
Kagoshima University, 1-21-24 Korimoto, Kagoshima 890-0065, Japan

K. Józwiak  
Poznań University of Technology, Piotrowo 5, 60 450 Poznan, Poland

## Introduction

It has been reported (Amos 1952) that some wood species accumulating silica may not cause fast tool dulling. In contrast, excessive cutting tool dulling was evidenced for some wood species which did not accumulate silica. Moreover, a comprehensible dissimilarity of the tool dulling progress while processing wood species of moderate climate zone (which practically do not accumulate silica) has also been described (Amos 1952).

Recent work has shown evidences linking rapid tool dulling during wood machining to the high-temperature corrosivity (HTC) and hard mineral contamination (Porankiewicz et al. 2003). In this paper the effect of six new wood species on the dullness progress of high-speed steel (HSS) tool after longitudinal cutting is discussed.

## Materials and methods

Wood specimens used in the experiment are listed in Table 1.

Milling conditions of the oil palm wood are described in an earlier work (Porankiewicz et al. 2005). The milling of nogal wood was performed at a cutting depth of  $g_S = 2$  mm (Bermudez et al. 2005), while other conditions remained the same as for oil palm. The routing of wood specimens 2–5 was performed under the following conditions: cutting edge made of SKH51 steel, RPM = 14,285; cutting speed  $v_C = 9.2$  m/s; number of cutting edges  $z = 2$ ; feeding rate per tooth  $f_Z = 0.05$  mm; rake angle  $\gamma_F = 10^\circ$ ; clearance angle  $\alpha_F = 15^\circ$ ; cutting depth  $g_S = 5$  mm; moisture content MC = 12–16% (Darmawan et al. 2003). The procedure of evaluation of hard mineral contamination (silica content) of wood specimens as well as contamination particles characterization is described in this work (Porankiewicz et al. 2005).

Figure 1 presents one corrosion peak on a plot of first derivative of mass against time during thermal analysis (dTG), employed for estimation of a  $R_{MW}$  quantifier, expressing the HTC effect of wood on iron. Every temperature  $T$  corresponds to a defined time  $t$ , due to constant temperature rise ( $\Delta T = 50^\circ/\text{min}$ ) set in Shimadzu TGA50 apparatus. The iron particles used in the TGA were approximately 2.5  $\mu\text{m}$  in diameter, according to the Functional Spectral Signature (FSS) method. More details concerning the methodology

**Table 1** Wood specimens used in the experiment

No.	Common name	Scientific name	Country of origin	Wood density ( $\text{kg}/\text{m}^3$ )
1	Oil palm	<i>Elais guineensis</i>	Indonesia	395
2	Coconut	<i>Cocos nucifera</i>	Indonesia	550
3	Teak	<i>Tectona grandis</i>	Indonesia	669
4	Red meranti	<i>Shorea</i> sp.	Indonesia	847
5	Passang	<i>Quercus</i> sp.	Japan	911
6	Nogal	<i>Cordia alliodora</i>	Columbia	482

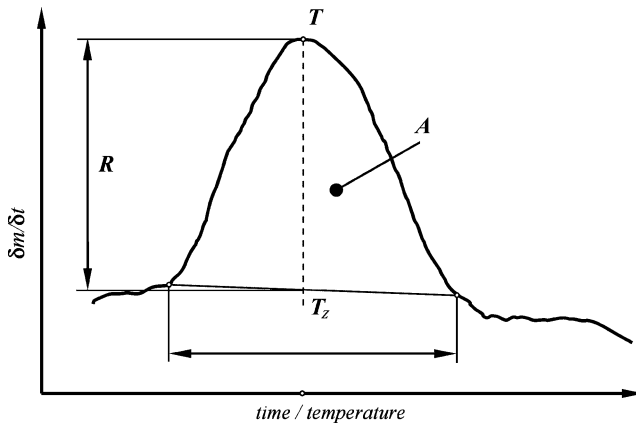


**Fig. 1** Parameters of the single corrosion peak from the dTG plot used for evaluation of the  $R_{MW}$  quantifier

of the HTC evaluation were described in an earlier work (Porankiewicz et al. 2005). The  $R_{MW}$  quantifier, defined by Eq. 1, was applied for quantification of the HTC of wood towards Fe. Variables of Eq. 1 are shown in Fig. 1:

$$R_{MW} = \frac{\sum (RTAT_z)}{m \sum T \sum A \sum T_z}, \quad (1)$$

where  $R$  is the height of a single corrosion peak on the dTG plot (mg/min),  $T$  the temperature of a single corrosion peak maximum ( $^{\circ}\text{C}$ ),  $\sum T$  the summation of single corrosion peak maxima ( $^{\circ}\text{C}$ ),  $A$  the area of a single corrosion peak,  $\sum A$  the summation of area of all corrosion peaks,  $T_z$  the temperature range of a single corrosion peak on the TGA plot ( $^{\circ}\text{C}$ ),  $\sum T_z$  the summation of temperature ranges  $T_z$ ,  $m$  the mass of iron specimen (mg) and dTG is the first derivation of iron mass ( $m$ ) increase during time  $t$ .

The  $R_{MW}$  is a weighted average mass increase speed of the iron specimen, considered in the corrosion peaks on the dTG plot within a temperature range of 210–570 $^{\circ}\text{C}$  (Fig. 1).

The cutting edge recession was measured on the clearance surface  $\text{VB}_F$ . More details concerning the evaluation of cutting edge profiles were described earlier (Porankiewicz et al. 2005).

Numerical analysis of the experimental data was performed by applying an algorithm based on the modified theoretical simulation method developed by Porankiewicz (1993, 2004). A quality of approximation of the theoretical model was characterized by SK, the summation of square of residuals as well as a square of the correlation coefficient  $R^2$ .

## Results and discussion

In Table 2, relative  $R_{MW}^W$  quantifier describing HTC of wood towards iron, total silica content ( $C_{MC}$ ) and content of silica in fractions  $f_1$ – $f_7$  for wood

specimens examined are collected. An exceptionally high value of  $R_{MW}^W$  for oil palm wood (specimen 1) is noteworthy.

The content of hard mineral contamination in wood examined here differs significantly (Table 2). Oil palm wood appeared to be the most mineral contaminated. Measurements performed showed that 90% of silica particles were smaller than 20  $\mu\text{m}$  (fraction  $f_7$ ). Most silica grains found in specimen nos. 1 and 2 were of spheroidal shape, large aggregates were also observed (Fig. 2). The presence of such aggregates was reported in previous works (Amos 1952; Porankiewicz et al. 2005). Small grains detected in specimens 1 and 2 were light gray-brown, nevertheless several grains found in specimens 3–6 were white, light brown or black. The black grains seemed to be not fully burned coal. Therefore, the procedure of combusted method for the evaluation of mineral contamination was expanded by adding 30 min of burning of the collected remains together with the glass filter at a temperature of 560°C. This step resulted in 5–15% of weight loss of the mass of mineral contamination. Large amount of black grains disappeared. The content of hard mineral contamination for specimens 4 and 5 evaluated in the present work (Table 2) differs significantly compared to values reported in another work (Darmawan et al. 2003).

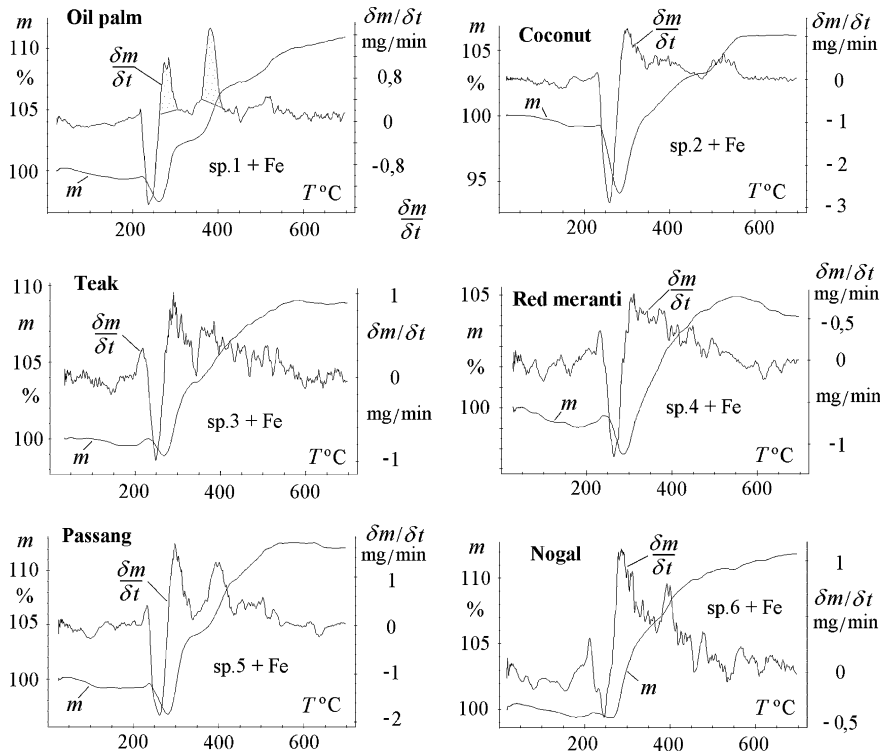
It can be seen from Fig. 2b that grains of mineral contamination of specimen 3 were pipe-like. Such morphology was not reported as yet. For further analysis, the shape of contamination particles was assumed isomeric, with the average grain size corresponding to the finest fraction.

Figure 3 shows the TGA plots (illustrating mass  $m$  changes) and the dTG plots (illustrating first derivation of mass against time  $\delta m/\delta t$ ) for the examined specimens. From Fig. 3 the  $R_{MW}$  quantifiers according to Eq. 1 were evaluated. The presence of two high and wide corrosion peaks for oil palm wood can be seen in Fig. 3 while numerous narrow and small peaks are shown for the others. In earlier works (Porankiewicz 2003; Porankiewicz et al. 2005) a strong correlation between high/wide corrosion peaks and the cutting edge wear was found, while for small/narrow peaks, together with slow increasing tendency of the  $\delta m/\delta t$ , such a correlation was not evidenced.

**Table 2** The high-temperature corrosivity expressed by relative  $R_{MW}^W$  quantifier and the content of silica  $C_{MC}$  in analyzed wood specimens

Specimen no.	$R_{MW}^W$	Total $C_{MC}$ (mg/kg)	Hard mineral contamination $C_{MC}$ (mg/kg) in						
			$f_1$	$f_2$	$f_3$	$f_4$	$f_5$	$f_6$	$f_7$
1	246.3	5,911.4	0	0	14.4	39.9	115.0	542.9	5,199.2
2	2.1	1,540.6	0	0	0	15.0	4.3	19.3	1,501.9
3	1.0	2,573.8	–	–	–	–	–	–	–
4	3.2	1.7	0	0	0.03	0	0	0	1.67
5	21.8	8.1	0	0.2	0	0	0	0	7.9
6	1.7	8.8	0	0.2	0	0	0	0	7.6

$f_1 > 0.6$ ;  $0.4 < f_2 \leq 0.6$ ;  $0.2 < f_3 \leq 0.4$ ;  $0.1 < f_4 \leq 0.2$ ;  $0.075 < f_5 \leq 0.1$ ;  $0.05 < f_6 \leq 0.075$ ;  $f_7 < 0.05$  (mm)



**Fig. 2** Particles of hard mineral contamination: **a** 3D aggregates from oil palm, specimen no. 1; **b** pipe-like grains from teak, specimen no. 4

The EDS analysis showed that silicon was the main element of contamination aggregates found in oil palm wood (Fig. 2a). Si was also the main element of pipe-like grains detected in teak wood (Fig. 2b). The pipe walls were thin enough, less than  $0.1\ \mu\text{m}$ . EDS analysis of the ash treated with hydrochloric acid showed the presence of calcium, potassium, magnesium and phosphorus. Large amounts of potassium and calcium were detected in oil palm and coconut specimens. Similar proportions of K and Ca have been reported in EDS results of keirung (*Combretocarpus* sp.) examined in a previous experiment (Porankiewicz et al. 2005). It is known that the high presence of K causes a decrease of the ash melting temperature, which might be a reason for the formation of aggregates of silica contamination during burning process. This hypothesis supports many cracks observed on the surface of the aggregates (Fig. 2a). It should also be noticed that the aggregates were only found in wood species nos. 1 and 2. In this context it can be stated that the combustion method of evaluation of hard mineral contamination seems to be not fully suitable for wood species containing large amounts of K and/or Ca. The amount of phosphorus in oil palm and coconut wood was large, comparable with the content of calcium. In the ash of red meranti

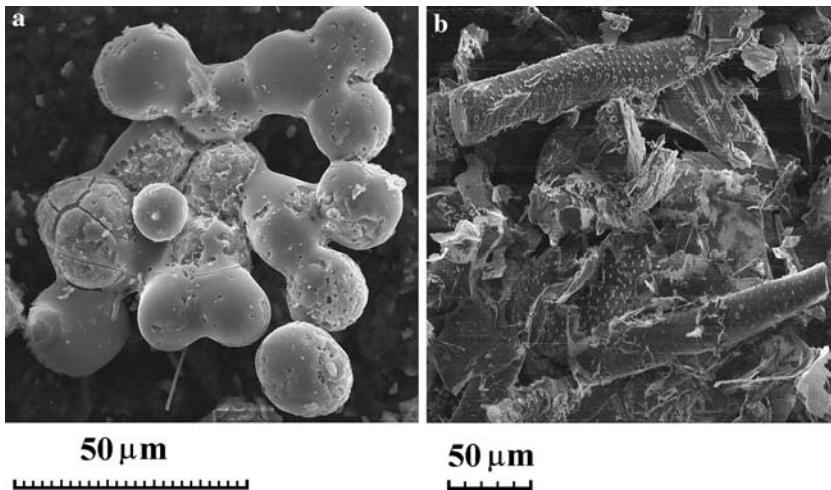


**Fig. 3** The TGA ( $m$ ) and the dTG ( $\delta m/\delta t$ ) plots of Fe together with wood specimens tested

(no. 4) and teak wood (no. 3) extraordinary high content of P was also detected. Large amount of Mg was found in ashes of oil palm and teak.

Figure 4 shows the SEM images of wood specimens analyzed. Some cyclic patterns can be seen on the surface of specimens 1–5. Rounded bulges proved not to be silica contamination particles. Unfortunately, the hard mineral contamination grains cannot be directly recognized using SEM/EDS technique as was expected.

In Table 3, the cutting wear data from three total cutting paths are gathered. In the first column, clearance surface cutting edge recessions  $VB_F$  for total cutting path  $L_S = 11,530$  m taken from an experiment by Darmawan et al. (2003) are reported. The next two columns show the cutting edge recessions  $VB_F$  for total cutting path  $L_S = 40,861$  m and  $L_S = 20,000$  m obtained after milling of nogal and oil palm wood, respectively. The largest observed cutting edge recession ( $VB_F = 142$   $\mu\text{m}$ ) was obtained for routing of the specimen no. 1. The largest wear could be associated with the highest hard mineral contamination:  $C_{MC} = 5,911.3$  mg/kg (see Table 2). However, at the same time, relatively high mineral contaminated wood of coconut (Table 2,  $C_{MC} = 1,540.6$  mg/kg) resulted in the lowest cutting edge wear rate ( $VB_F = 69$   $\mu\text{m}$ ). Moreover, rather high cutting edge wear rate was also observed in the case of passang wood with almost no silica contamination (Table 2,  $C_{MC} = 8.8$  mg/kg). The above-mentioned remarks imply that a fundamental abrasion role of natural silica on the cutting edge wear is not evident.

The cutting edge wear data indicate that although the routing of oil palm was realized at distinctly lower cutting speed, as high as 9.2 m/s (compared to 30 m/s at milling), the wear rate was over 20% higher at almost a half of the cutting path  $L_S$  during milling. Therefore, it can be concluded that the cutting edge wear is much faster during routing. This observation could be linked to the lower tool stiffness and higher vibrations of the routing bit. A uniform

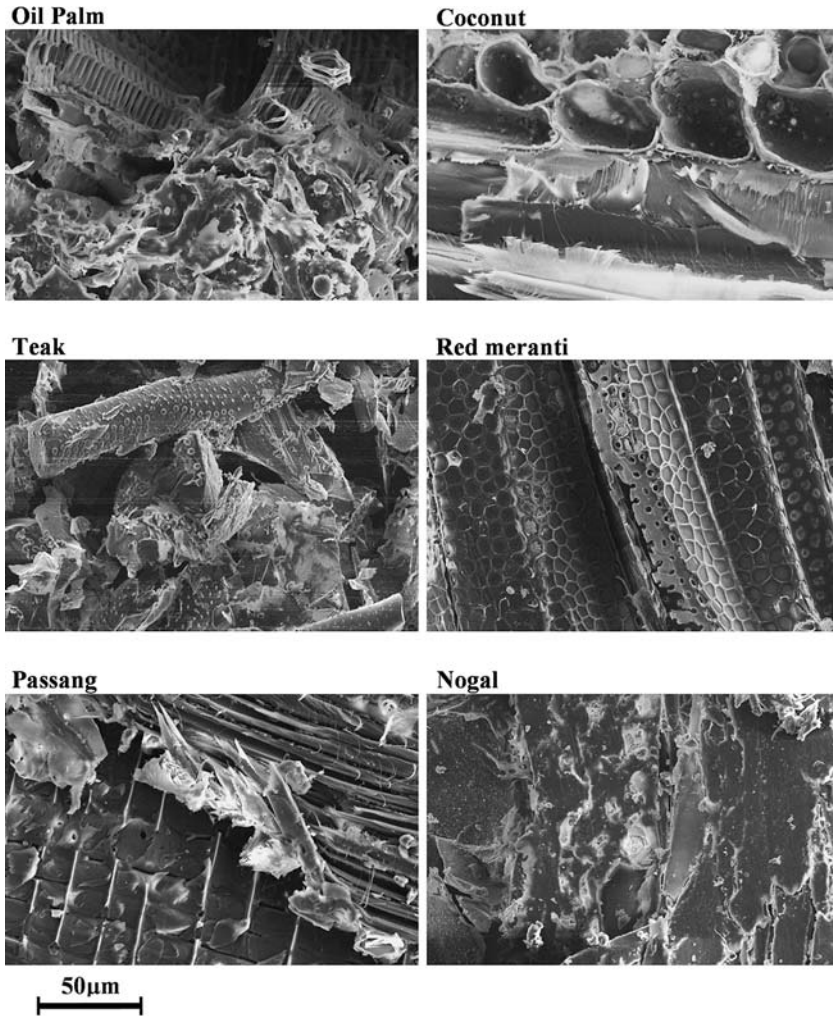


**Fig. 4** SEM images of wood specimens tested

**Table 3** Clearance surface cutting edge recession  $VB_F$  for wood specimens after routing (r) and milling (m), after different cutting paths  $L_S$

Specimen	$L_S = 11,530$ m	$L_S = 40,861$ m	$L_S = 20,000$ m
1. Oil palm	142 <sup>r</sup>	–	114.8 <sup>m</sup>
2. Coconut	69 <sup>r</sup>	–	–
3. Teak	77 <sup>r</sup>	–	–
4. Red meranti	77 <sup>r</sup>	–	–
5. Passang	103 <sup>r</sup>	–	–
6. Nogal	–	73 <sup>m</sup>	–

Routing (r) values are taken from Darmawan et al. (2003)

pattern of the worn area of the cutting edge can be seen on the clearance surface of the tool after oil palm cutting, which is in agreement with a lack of big size contamination grains (Table 2,  $f_1$  and  $f_2$ ). The lowest cutting edge wear  $VB_F$  for almost not mineral contaminated nopal wood was observed. This particularly low tool wear is connected to the low HTC and wood density  $D$ .

The data from Tables 1 and 2 were correlated with the cutting edge wear rate observed and collected in Table 3. The silica content and the HTC are overlapping effects for specimen no. 1. In this case a remarkable synergistic effect of mechanical and HTC wear probably occurred.

Although the wood densities differ significantly (395 vs. 910 kg/m<sup>3</sup>) the cutting edge wear  $VB_F$  and wood density  $D$  do not follow each other. An exception might be for passang wood (specimen 5), with its highest density  $D$  and large relative  $R_{MW}$  quantifier. Since no direct correlation of the cutting edge wear  $VB_F$  with content of silica  $C_{MC}$  and wood density  $D$  was established, an attempt of multi-parameter analysis using data from Table 3 was undertaken. Results of computations for the model, based on results taken from Darmawan et al. (2003), without pipe-like contamination grains, showed that assuming the HTC, silica content  $C_{MC}$ , particles size  $S_{CP}$  and wood density  $D$  effects, the correlation coefficient between predicted wear rate  $VB_F^P$  and the wear rate observed  $VB_F$  was as high as  $R^2 = 0.989$  by summation of residuals square  $SK = 387.4$  (Fig. 5). The model approximated for the presence of pipe-like grains was worse, reaching  $SK = 423.8$  showing low influence of such unusual contamination grains on the cutting edge wear.

Taking into account the model evaluated for results of Darmawan et al. (2003) (Fig. 6a), it was found that for oil palm, the average contribution of the HTC and the silica contamination  $C_{MC}$  on the cutting edge wear are as high as 69 and 5.5%, respectively. The HTC expressed by the  $R_{MW}$  quantifier appeared to be a very essential factor influencing the HSS cutting edge wearing for all woods investigated.

Analyzing a model evaluated for previous results (Porankiewicz et al. 2005) expanded by oil palm wood (Fig. 6b), it can be seen that the separated contribution of the HTC and the silica contamination to the cutting edge wear

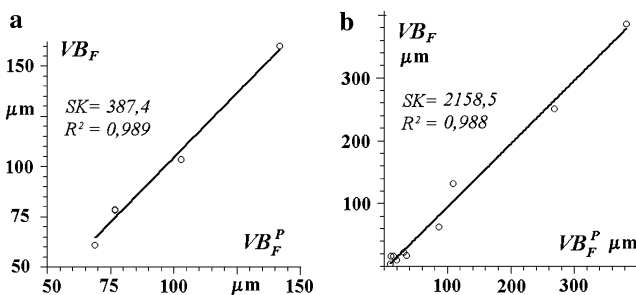


**Fig. 5** Correlations between predicted  $VB_F^P$  and observed  $VB_F$  tool wear for models: **a** based on data from Darmawan et al. (2003); **b** obtained from data of Porankiewicz et al. (2005), expanded by oil palm wood



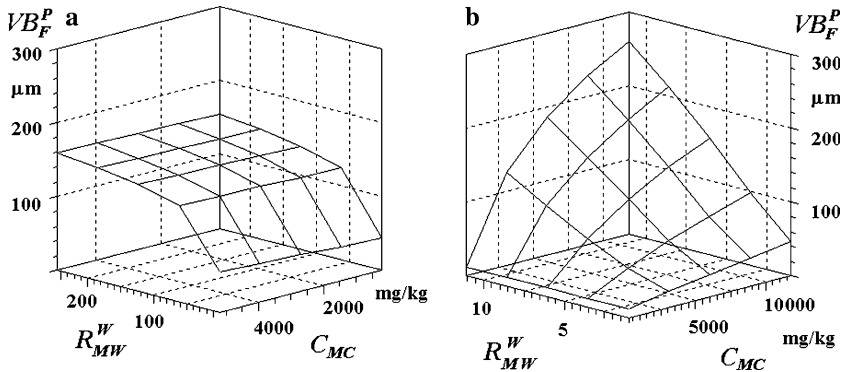


**Fig. 6** The dependence of the cutting edge wear  $VB_F^P$  on silica content  $C_{MC}$  and  $R_{MW}^W$  relative quantifier for: **a**  $D = 650 \text{ kg/m}^3$ ,  $S_{CP} = 25 \text{ }\mu\text{m}$ ; **b**  $D = 395 \text{ kg/m}^3$ ,  $S_{CP} = 25 \text{ }\mu\text{m}$

was low, and the dominant role in the cutting edge wear resulted from synergistic effect of the two factors, reaching 82%. Tendencies presented in Fig. 6a, b are contradictive. More investigations are needed for better description and explanation of the wear process examined in this work.

## Conclusions

1. The fundamental, abrasion role of the low size natural silica grains on the cutting edge wear has not been evidenced in this study.
2. Results of the multi-parameter simulation showed that the most influencing factor on the HSS tool wear was the HTC, with a synergistic effect together with low size natural silica contamination grains.
3. The lowest tool wear was observed for nogal wood, exhibiting low HTC, low mineral contamination  $C_{MC}$  and low density  $D$ .
4. Almost 90% of spheroidal hard mineral contamination grains found in oil palm and coconut wood specimens were less than  $20 \text{ }\mu\text{m}$ .
5. The presence of large aggregates among contamination grains, found in oil palm and coconut ashes, might be associated with the high quantity of potassium and calcium, significantly dropping down the ash melting temperature.
6. Most of the silica mineral contamination grains of teak wood were of thin-walled pipe-like morphology.
7. The analyses performed show that pipe-like grains play a smaller role in the cutting edge wear than typical spheroidal ones.
8. Third burning of the ash remaining on a glass filter has to be included into the procedure of the combustion method of hard mineral contamination.

**Acknowledgments** Theoretical simulation calculations were performed at Poznań Supercomputing-Net Center PCSS. Some part of this research has been performed during post doc financed by *Provincia Autonoma di Trento*, Italy.

## References

- Amos GL (1952) Silica in timbers, no. 267. CSIRO, Australia, p 61
- Bermudez J, Ohtani T, Tanaka C (2005) The machinability of nogal (*Cordia alliodora*) grown in Colombia. *J For Biomass Use Soc*:7 (in press)
- Darmawan W, Tanaka C, Svoradova M, Marchal R (2003) Chemical and mechanical wearing of high speed steel and tungsten carbide by some Indonesian woods. In: Proceedings of the 16th international wood machining seminar (IWMS), Shimane University, Matsue, Japan, pp 487–493
- Porankiewicz B (1993) Catastrophic wear mechanism when milling particle board. In: Proceedings of the 11th IWMS, Oslo, Norway, pp 509–514
- Porankiewicz B (2003) A method to evaluate the chemical properties of particle board to anticipate & minimize cutting tool wear. *Wood Sci Technol* 37(1):47–58
- Porankiewicz B (2004) Theoretical simulation of cutting edge wearing when wood and secondary wood products cutting. *Wood Sci Technol*:11 (in press)
- Porankiewicz B, Sandak J, Tanaka C (2003) The HSS tool wear when milling wood. In: 16th IWMS, Matsue, Japan, vol 2, pp 494–502
- Porankiewicz B, Sandak J, Tanaka C (2005) Factors influencing steel tool wear when milling wood. *Wood Sci Technol* 39(3):225–234